

# Can HII regions be older than we thought?

TBD,<sup>1</sup>★  
<sup>1</sup>TBD

Accepted XXX. Received YYY; in original form ZZZ

## ABSTRACT

**Key words:** keyword1 – keyword2 – keyword3

## 1 INTRODUCTION

McLeod et al. (2019) (M19 thereafter)

- hii regions important - refs?
- ages determination important -refs ?
- loads of different methods to get age: WHAT ARE THEY?
- here trying to work out/test unresolved ages from emission lines with a resolved stellar population, i.e. we can see the stars in 118 and 119 - work out ages and test nebular emission back against what we also detect in the same regions - check ionizing flux output and stellar mass too or something

## 2 OBSERVATIONS AND MODELS

### 2.1 Observational Data

**TALK ABOUT THE INDIVIDUAL HII REGION NAMES ABC ETC... ?? DECIDE LATER WHEN MORE HAS BEEN WRITTEN** The stars considered in this work (see Table 1) belong to two giant HII region complexes – D118 and D119 – located within NGC 300 (D~2 Mpc,  $Z=0.33Z_{\odot}$ ). We remark that the D118 and D119 notation is an abbreviation of the format established by Deharveng et al. (1988) introduced in M19. For consistency with table 3 of M19, however, we conserve the original nomenclature in our Table 1. They were observed by M19 using the Multi Unit Spectroscopic Explorer (MUSE – Bacon et al. 2010) on the Very Large Telescope, and high angular resolution Hubble Space Telescope catalogues were used to deblend and resolve single stars. Further details on the observations and the data reduction can be found in Section 2 of M19.

In order to derive stellar parameters, M19 fitted the extracted spectra of each star to PoWR atmosphere model grids. As they were solely calculated for Galactic, LMC and SMC metallicities, and given that for NGC 300  $Z \approx 0.33Z_{\odot}$  Butcher et al. (2004), the LMC PoWR grids ( $Z =$

$0.5Z_{\odot}$ ) were the most consistent. The best fit were identified using  $\chi^2$  minimisation. One major source of uncertainty is that unresolved binaries are not taken into account – photon fluxes calculated are therefore lower limits. Additionally, the limited number of strong WR star features in the spectra of two of the 4 WR stars observed by M19 led to unconstrained stellar parameters. Therefore they cannot be used in this work.

In the case of 119-3, the stellar parameters derived from the initial PoWR model fits yielded a mass ( $15.7M_{\odot}$  – see table 2 MC19) that is too low to explain the prominent He II  $\lambda 5411$  lines seen in the spectrum of this source. Focusing on the He II  $\lambda 6406$  line for their PoWR fits, they re-evaluate the luminosity and mass of 119-3. In this work we consider both sets of stellar parameters: 119-3 and 119-3b, corresponding to the original and revised parameters, respectively.

### 2.2 BPASS and hoki

The Binary Population and Spectral Synthesis –BPASS– models simulate the evolution of stellar populations for a range of metallicities and initial mass functions (IMFs) with the ability to take into account the effects of binary populations. An exhaustive description of the physical prescriptions included in the models can be found in Eldridge et al. (2017); Stanway & Eldridge (2018). In this work we use the outputs of BPASS v2.2.1 with a standard IMF (Salpeter 1955) and a metallicity  $Z = 0.06$  corresponding to  $\approx 1/3 Z_{\odot}$ , which is the closest BPASS metallicity to NGC 300. We also consider  $Z = 0.08$  and  $Z = 0.10$  (i.e.  $0.4Z_{\odot}$  and  $0.5 Z_{\odot}$ ) since the physical parameters of the stars in M19 were found based on  $Z = 0.5Z_{\odot}$  PoWR models. We discuss the effects of varying metallicity in Appendix ??.

**YO METALLICITY MATTER FOR MASS AND STELLAR COUNTS< NEEDS TO HAPPEN IN TEXT AS WELL- ONLY PUT THE EXTRA PLOTS IN APPENDIX**

The data analysis based on the BPASS outputs was performed using hoki v1.2.1-beta<sup>1</sup> (Stevance et al in prep.),

★ E-mail: TBD

<sup>1</sup> <https://github.com/HeloiseS/hoki>

**Table 1.** Stellar parameters for the O-type and WR stars considered in this work as obtained by M19 (see their tables 3 and 4) from best-fit PoWR atmosphere models (Hainich et al. 2019). The most likely age of each star according to the probability distribution functions inferred from the synthetic HRDs of BPASS are also given – the non-gaussian nature of most of these distributions does not allow us to provide errors bars and we refer the reader to Figure A1. Note that the 119-3 and 119-3b stellar parameters refer to the same source but correspond to two different PoWR model fits – for further details see text in Section 2.1

ID	log(L) ( $L_{\odot}$ )	log(T) ( $T_{\odot}$ )	Most likely age log(years)			P( $6.7 \leq \log(\text{age}) \leq 6.9$ )		
			Z=0.06	Z=0.08	Z=0.10	Z=0.06	Z=0.08	Z=0.10
[DCL88]118-1	5.0	4.48	6.9	6.8	6.8	88.1 %	81.3 %	60.9 %
[DCL88]118-2	5.1	4.45	6.7	6.7	6.7	95.7 %	76.2 %	68.7 %
[DCL88]118-3	4.9	4.46	6.8	6.8	6.8	80.3 %	67.4 %	57.6 %
[DCL88]118-4	5.9	4.47	6.5	6.5	6.5	12.7 %	13.5 %	9.5 %
[DCL88]118-WR2	5.3	4.9	6.9	6.8	6.8	87.3 %	73.7 %	97.2 %
[DCL88]119-1	5.0	4.48	6.9	6.8	6.8	88.1 %	81.3 %	60.9 %
[DCL88]119-2	5.4	4.53	6.7	6.7	6.7	98.1 %	76.0 %	58.8 %
[DCL88]119-3	4.3	4.52	6.8	6.7	6.7	57.3 %	47.3 %	36.3 %
[DCL88]119-3b	5.7	4.52	6.7	6.5	6.5	70.4 %	28.9 %	17.2 %
[DCL88]119-4	4.5	4.52	6.9	6.9	6.9	61.2 %	58.1 %	54.8 %
[DCL88]119-5	4.5	4.56	7.3	7.3	7.3	3.7 %	3.1 %	3.8 %
[DCL88]119-6	4.9	4.46	6.8	6.8	6.8	80.3 %	67.4 %	57.6 %
[DCL88]119-7	4.5	4.52	6.9	6.9	6.9	61.2 %	58.1 %	54.8 %
[DCL88]119-8	4.3	4.52	6.8	6.7	6.7	57.3 %	47.3 %	36.3 %
[DCL88]119-9	4.5	4.52	6.9	6.9	6.9	61.2 %	58.1 %	54.8 %
[DCL88]119-WR1	5.3	4.65	6.9	6.9	6.9	84.5 %	81.3 %	76.3 %

a Python package designed to interface with BPASS outputs to facilitate data analysis and comparison to observational data. Jupyter notebooks showing the complete analysis contained within this paper have been made available online for reproducibility purposes<sup>2</sup>.

### 3 RESULTS

#### 3.1 Stellar age estimate from HRDs

One of the outputs of the BPASS models is an ensemble of Hertzsprung-Russell Diagrams (HRD) for each combination of IMF and Z covering 51 time bins ranging from  $10^6$  to  $10^{11}$  years<sup>3</sup>. Each pixel of a BPASS HRD grid contains a value representing the probability of a star being found in that particular location at a give age, IMF and metallicity.

Using the luminosities and temperatures inferred by M19 – see Table 1 – we can identify which grid element corresponds to each star. By considering all time steps, we can then build a probability distribution function (PDF) indicating the most likely age of a star found at a given location on the HRD.

Doing this for all stars listed in Table 1, we obtain the PDFs shown in Figures A1, A2 and A3, for  $Z = 0.06, 0.08$  and  $0.10$  (respectively). The most likely age peak of the distribution) for each star is also summarised Table 1.

Overall, most stars have similar preferred ages: between 5 and 8 Myrs ( $\log(\text{age})=6.7-6.9$ ). **SAY SOEMWHERE THAT PDFs GET BROADER** At  $Z = 0.06$ , only 118-4 and 119-5 deviate from this trend, being respectively younger (3 Myrs) and older (20 Myrs) than the rest of the population; the same most likely ages and very consistent PDFs are

found for these sources at  $Z = 0.08$  and  $0.10$ . Additionally, at  $Z = 0.08$  and  $0.10$  (half solar), 119-3b is also found to have a most likely age younger than the rest of the population ( $\log(\text{age})=6.5$ ), whereas at  $Z = 0.06$  it was consistent with the majority of our sources.

It is also interesting to note that the PDFs of at least one of the WR stars at all three metallicities will show a secondary probability peak between  $\log(\text{age}) \sim 8.0$ , which corresponds to 30 – 100 Myrs. This is an unphysical age range for a WR star and it must therefore correspond to another type of source that is found in a similar region of the HRD as WR stars.

We will first discuss these outliers before attempting to combine the individual PDFs to infer the most likely age of D118 and D119.

#### 3.2 Outliers

##### 3.2.1 118-4

As seen in the Figure A1, the position of 118-4 on the HR diagram correspond to a most likely age that is younger ( $\log(\text{age})=6.7$  years, equivalent to  $\sim 3$  Myr) than all other stars in D118 and D119, which typically prefer ages around 5–8 Myrs. The asymmetric probability distribution functions of some stars in our sample do extend down to very early ages that overlap with 118-4 – that is the case for 119-3,4,7,8 and 9. However, if we calculate the probability that a star has a  $\log(\text{age})$  between 6.7 and 6.9 years, we can see that all of these other targets have  $\sim 60-70$  per cent chance of being in that age range, whereas 118-4 only has a 3.7 per cent probability. Consequently, it is highly likely that 118-4 genuinely is, or *appears*, younger.

If we consult MC19, particularly their Figure 5, we can see that 118-4 is located away from most stars in D118, which could indicate that it formed at a slightly later date.

<sup>2</sup> LALALALA

<sup>3</sup> Note that the bins are uniformly distributed in  $\log(\text{age})$  space

However, 118-2 and 118-WR2 are also somewhat isolated, and their most likely ages are consistent with the other stars in this region.

Another way to explain the youthful appearance of 118-4 is through rejuvenation: if the star underwent a merger event, or accreted a substantial amount of material from a binary companion, it would present as a younger star (REF). The fact that MC19 find this source to be the most massive in their sample count hint that it is the result of a stellar merger.

### 3.2.2 119-3b

The PDF of the age of the 119-3b stellar parameters evolve to prefer lower ages ( $\log(\text{age})=6.5$ ) as metallicity increases (WHY).

Overall, the PDF and preferred age of 119-3b are similar, to 118-4. This is consistent with the derived masses (41.3 and 49.2  $M_{\odot}$  for 119-3b and 118-4, respectively – see table 2 MC19), which are significantly higher than for the other sources in the sample. The greater mass of 118-4 compared to 119-3b also explains why the shape of age distribution is more pronounced towards lower ages.

**JJ WRITE A THING! BAOUT MEGERS, AGES, REJUVINATION AND BPASS SHENANIGANS.**

### 3.2.3 119-5

Contrary to 118-4, 119-5 appears much older than the other sources in our sample, with most likely  $\log(\text{age})=7.3$  years ( $\sim 20$  Myrs) which is too old for a source in an H II region. In Figure 9 of MC19 we can see that 119-5 is located away from the core of 119-A inhabited by 119-3,4,6,8 and 9. Either background or foreground star, or something is lowering temperature and luminosity => DUST? **COULD THIS BE BACKGROUND OR FOREGROUND? ASK ANNA AGAIN**

### 3.2.4 WR stars at 100 Myrs?

As mentioned in Section 3.1, more than half of the age PDFs recovered for the WR star locations on the HRD show a secondary probability peaks between  $\log(\text{age})=7.5$  and 8.0 (see Figures A1, A2 and A3). This does not impact our ability to recover a sensible age for WR stars: at all metallicities both 118-WR2 and 119-WR1 have at least a  $\sim 70$  per cent (up to 97 per cent) probability of having an age between  $\log(\text{age})=6.7$  to 6.9  $\sim 5-8$  Myrs).

The secondary probability surge at later ages can be explained by the presence of helium star in the BPASS models which are found in the same region of the HRDs but at later times. These therefore do not correspond to WR stars but will appear in the age PDFs corresponding to their stellar parameters  $\log(T)$  and  $\log(L)$ .

## 3.3 Aggregate age

In order to estimate the age of D118 and D119 we multiply the PDFs of the stars in these regions. We choose not to include the outliers in our sample, that is: 118-4, 119-5 and

**Table 2.** Total mass, star count and expected W/O star ratio for the D118 and D119 clusters at the preferred ages identified in Section 3.3 and the metallicity of NGC 300 ( $Z = 0.06$ ).

Age $\log(\text{years})$	$\log(M_{\text{tot}})$ $M_{\odot}$	Star Count ( $\times 10^3$ )	WR/O
6.7	$3.62^{+0.15}_{-0.23}$	$8.3 \pm 3.4$	0.08
6.8	$3.80^{+0.13}_{-0.23}$	$12.7 \pm 5.2$	0.15
6.9	$4.30^{+0.13}_{-0.23}$	$39 \pm 16$	0.73

119-3b. Additionally, 119-3 represents a different sets of parameters for the same source as 119-3b, but as demonstrated in MC19, the 119-3b stellar parameters are more suited to fit the target. Therefore we also omit the 119-3 PDF from the aggregate as it is not actually representative of the source in our sample.

In Figure 1 we present the PDFs of the ages of D118, D119, and the whole region, based on our sample and BPASS models at  $Z = 0.06, 0.08$  and 0.10. For each region-metallicity pair, we include an age PDF calculated including and excluding the WR stars in the sample. Indeed, the position of the WR stars on the HRD gives them quite narrow PDFs which can drastically change the shape of the aggregate PDFs. In the case of D118 ( $Z = 0.06$ ), for example, the inclusion of WR stars even brings the probability of the  $\log(\text{age})=6.7$  bin to zero. Overall, the inclusion of the WR stars tends to narrow the aggregate PDFs for the ages of our HII regions.

Given the uncertainties on the temperature estimates of WR stars, caution is required when extreme changes to the PDF are caused by the inclusion of these stars in the sample. For example, it is probably not reasonable to conclude that the  $\log(\text{age})=6.7$  bin must be excluded excluded for D118 ( $Z = 0.06$ ) solely based on the inclusion of one WR star.

The combined age of D118 and D119 is also sensitive to whether we include the WR stars in our sample or not, usually with a younger age associated with the exclusion of WR star (**isn't that counter-intuitive?**). The metallicity also seems to drive ages down **WHY? BECAUSE MORE STELLAR WINDS SO MORE STRIPPED SO BRIGHTER? that's a very single star mindset, JJ's gonna tut at me.**

Once again we want to emphasise that these distributions and their width is only representative of the BPASS models and does not take into account the uncertainties that may arise from stellar parameter fitting, and the great degree of precision observed in some PDFs in Figure 1 is not expected to be representative of true sources of noise. (ARE THERE SYSTEMATIC ERRORS WE SHOULD WORRY ABOUT?) Nevertheless, we can conclude from the good agreement between our aggregate PDFs that D118 and D119 likely have ages  $\sim 5 - 8$  Myrs ( $\log(\text{age})=6.7-6.9$ ).

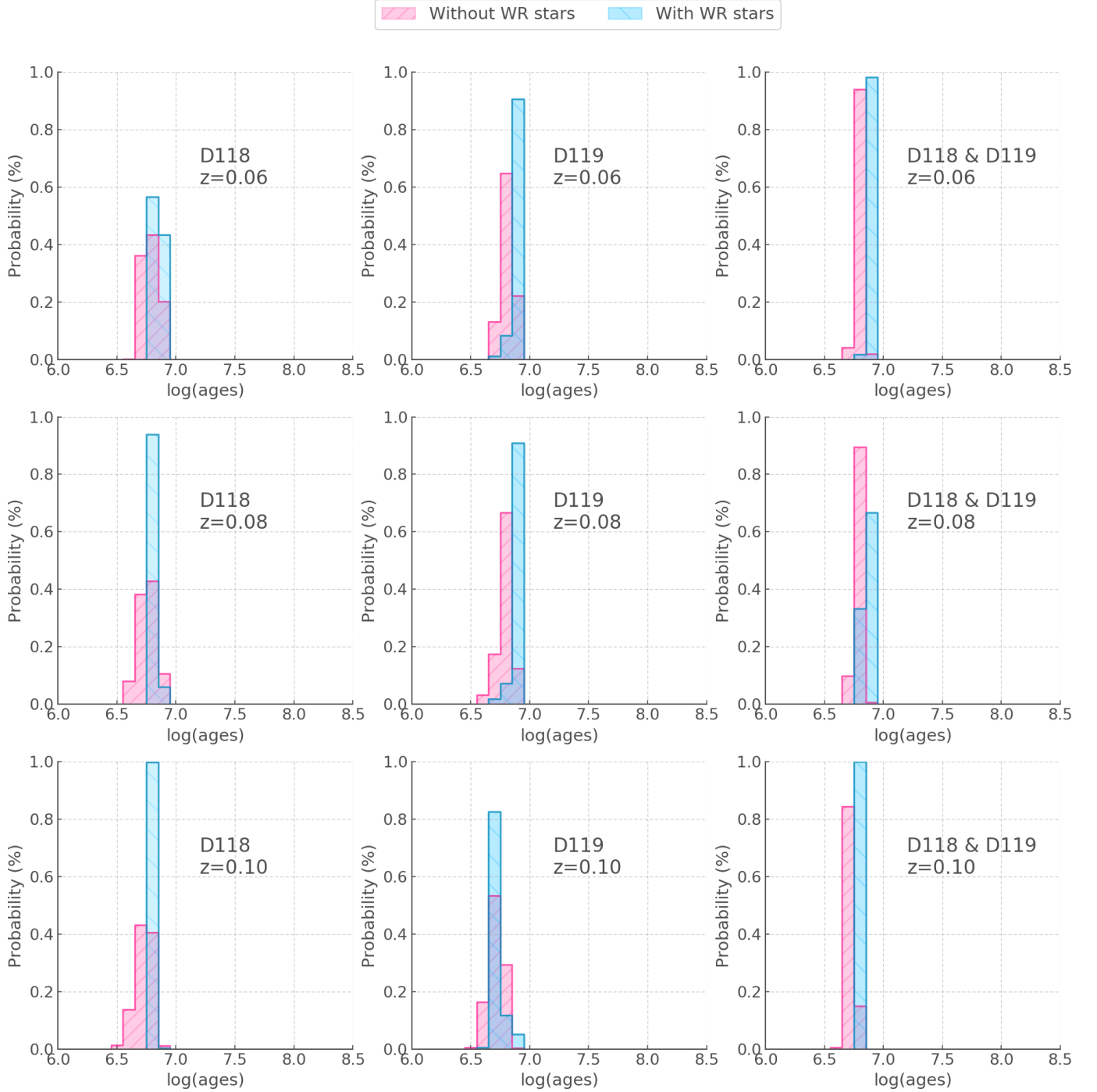


**Figure 1.** Probability distribution functions of D118 and D119 produced from the combination of the PDFs in Figure A1, not including 118-4, 119-5 or any of the 119-3 stellar PDFs.

#### 4 NOPE THIS DON'T MAKE SENSE THE FOLLOWING GOES WITH THE SECTION ABOVE TOO

##### 4.1 Stellar numbers: observations Vs theory

Based on the age of our systems, as determined in Section 3.3, we can search within our models to retrieve the number of O stars and WR stars we would expect to find. By comparing this to the number of O+WR stars observed we

can deduce the mass of the system by scaling the standard BPASS mass ( $10^6 M_{\odot}$ ). Additionally, we can independently calculate an age estimate by comparing the observed and expected WR to O star ratios.

We focus on  $\log(\text{age}) = 6.7, 6.8$  and  $6.9$ , as they were identified as the most likely ages for the D118 and D119 in Section 3.3, and summarise the total stellar mass and count obtained for the metallicity of NGC 300 ( $Z = 0.06$ ) in Table 2. We also provide the WR/O ratio for these ages.

It was important to take into account in these calculations that the observed number of stars is likely to be incomplete, as mentioned in M19. In order to mitigate the effects of incompleteness we choose to only compare the brightest members of the population. The BPASS outputs are provided separately for stars with  $\log(L) \geq 4.9$  and stars with  $\log(L) < 4.9$ . Since observations are less likely to suffer from incompleteness at the bright end of the luminosity range, we only consider stars with  $\log(L) \geq 4.9$ .

In both D118 and D119 four O stars meet this criteria. The two WR stars reported with stellar parameters in M19 also a high luminosity and it is safe to assume that the other two do as well. This results in an observed  $WR/O = 0.50 \pm 0.43$  for both D118 and D119, assuming Poisson errors. This corresponds to a  $\log(\text{age}) = 6.86^{+0.05}_{-0.26}$  and  $\log(M_{\text{tot}}) = 4.13^{+0.23}_{-0.45}$ .

## 4.2 Ionizing flux

Using ionizing-bin-z006 and values from M19 table 6

[So looking at table 6 of M19 we have ionizing fluxes for the two regions of 49.95 and 50.27, at the above ages this turns into log masses of  $4.35^{+0.17}_{-0.77}$  and  $4.67^{+0.17}_{-0.77}$ . These are consistent with the numbers, and also greater than the ionized gas mass derived from the nebula gas which is good as if they are later a lot of gas already expelled. So we are predicting the right H-alpha flux/number of ionizing photons.]

## 4.3 Predicted age and BPT diagrams

[needs a rewrite to point out that above is about correct number of photons, below is about the spectrum being correct]

A key way insight can be gained into a HII region are the various lines that are observed in an optical spectrum of the region in addition to those of the Balmer series of hydrogen. These provide greater information on the parameters of the ionized gas as well as the ionizing spectrum of the stars [e.g. refs]. We have taken the lines ratios used in the BPT diagram [ref] from M19 and compare these to the BPASS predictions of nebular emission for a population of the same age as we infer above.

We see in Figure 2 that the BPASS models are able to reproduce the observed line ratios at ages inferred for these regions above. However we must note that there is considerable degeneracy in the age for the binary populations. This is because binary interactions lead to the ionizing flux from the stars to last for extended periods of time as described by [xiao2018,2019]. In comparison for the single star populations we see that only models with an age of  $10^{6.7}$  years is able to match the observed line flux ratios. In addition this only occurs at the highest hydrogen gas densities.

We have only a limited number of observed lines but in attempting to find the best fitting model as in [xiao2018] is difficult and the uncertainties in age are significant. However we are able to find that the ionization parameter  $U$  has values in the range of -2.5 to -3 and the gas density of the regions in the range of  $\log(\rho/\text{g cm}^{-3}) = 2$  to 3. Part of the problem in deriving the age of the HII regions from the line ratios is that younger stellar populations can produce the

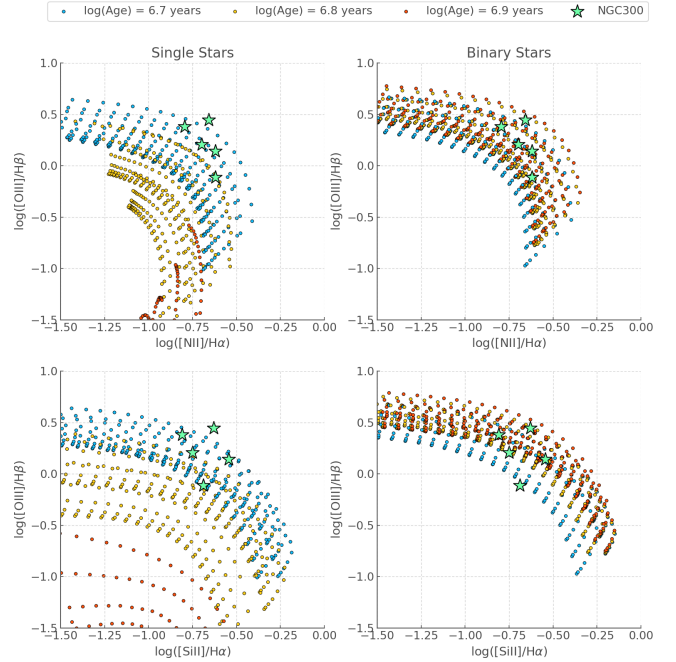


**Figure 2.** BPT diagram showing BPASS predicted lines ratios from [Xiao2018] and the line flux ratios for the HII regions 118a, 118b, 119a, 119b and 119c. The observed line ratios are shown by dark blue squares. The left-hand panels are for single star population models and the right-hand panel for the binary star predictions. For these tracks the ionization parameter,  $U$ , increases from left to right and the higher tracks of the same colour represent higher densities for the hydrogen gas around the stars. **z006 and z008 shown cuz 0.33solar met is in between**

line ratios of these regions. However at such ages the stellar populations predict no Wolf-Rayet stars or that the number of O stars significantly outnumber these stars which is clearly not the case. Thus we can discount such fits.

Our main finding here however is that our predicted nebula emission line ratios at the age of the stellar population derived from the resolved stellar populations is consistent with that observed. This provides a validation on the predicted BPASS nebula spectra. Also it confirms the hints in [Xiao2018] that some HII regions observed in other galaxies may in fact be significantly older than the frequently assumed upper age for a HII region of 3 Myrs.

## 5 DISCUSSION AND CONCLUSIONS

### ACKNOWLEDGEMENTS

lalalala Marsden Grant.

### REFERENCES

- Bacon R., et al., 2010, in Proc. SPIE. p. 773508, doi:10.1117/12.856027
- Butler D. J., Martínez-Delgado D., Brandner W., 2004, *AJ*, **127**, 1472
- Deharveng L., Caplan J., Lequeux J., Azzopardi M., Breysacher J., Tarengi M., Westerlund B., 1988, *A&AS*, **73**, 407

- Eldridge J. J., Stanway E. R., Xiao L., McClelland L. A. S., Taylor G., Ng M., Greis S. M. L., Bray J. C., 2017, [Publ. Astron. Soc. Australia](#), **34**, e058
- Hainich R., Ramachandran V., Shenar T., Sander A. A. C., Todt H., Gruner D., Oskinova L. M., Hamann W. R., 2019, [A&A](#), **621**, A85
- McLeod A. F., et al., 2019, arXiv e-prints, p. [arXiv:1910.11270](#)
- Salpeter E. E., 1955, [ApJ](#), **121**, 161
- Stanway E. R., Eldridge J. J., 2018, [MNRAS](#), **479**, 75

## APPENDIX A: PLOTS FOR NOW SO I DON'T PRINT THEM EVERY TIME

This paper has been typeset from a  $\text{\TeX/L}^{\text{A}}\text{\TeX}$  file prepared by the author.



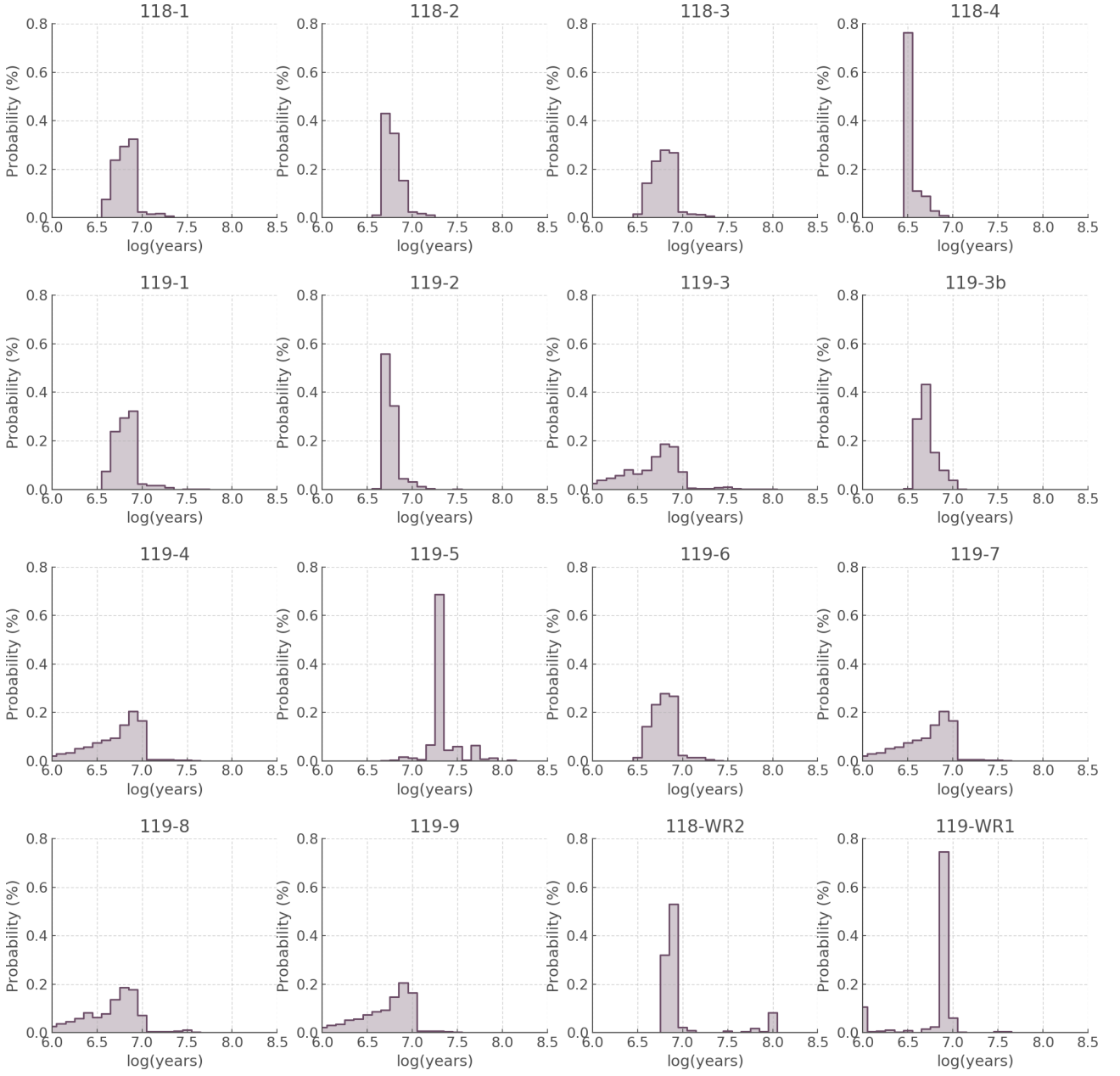


**Figure A1.** Probability distribution functions of the age of each star inferred from the stellar parameters quoted in Table 1 and the synthetic HRDs of BPASS for a standard IMF and a metallicity  $Z = 0.06$ . The most likely age of each star is summarised in Table 1.

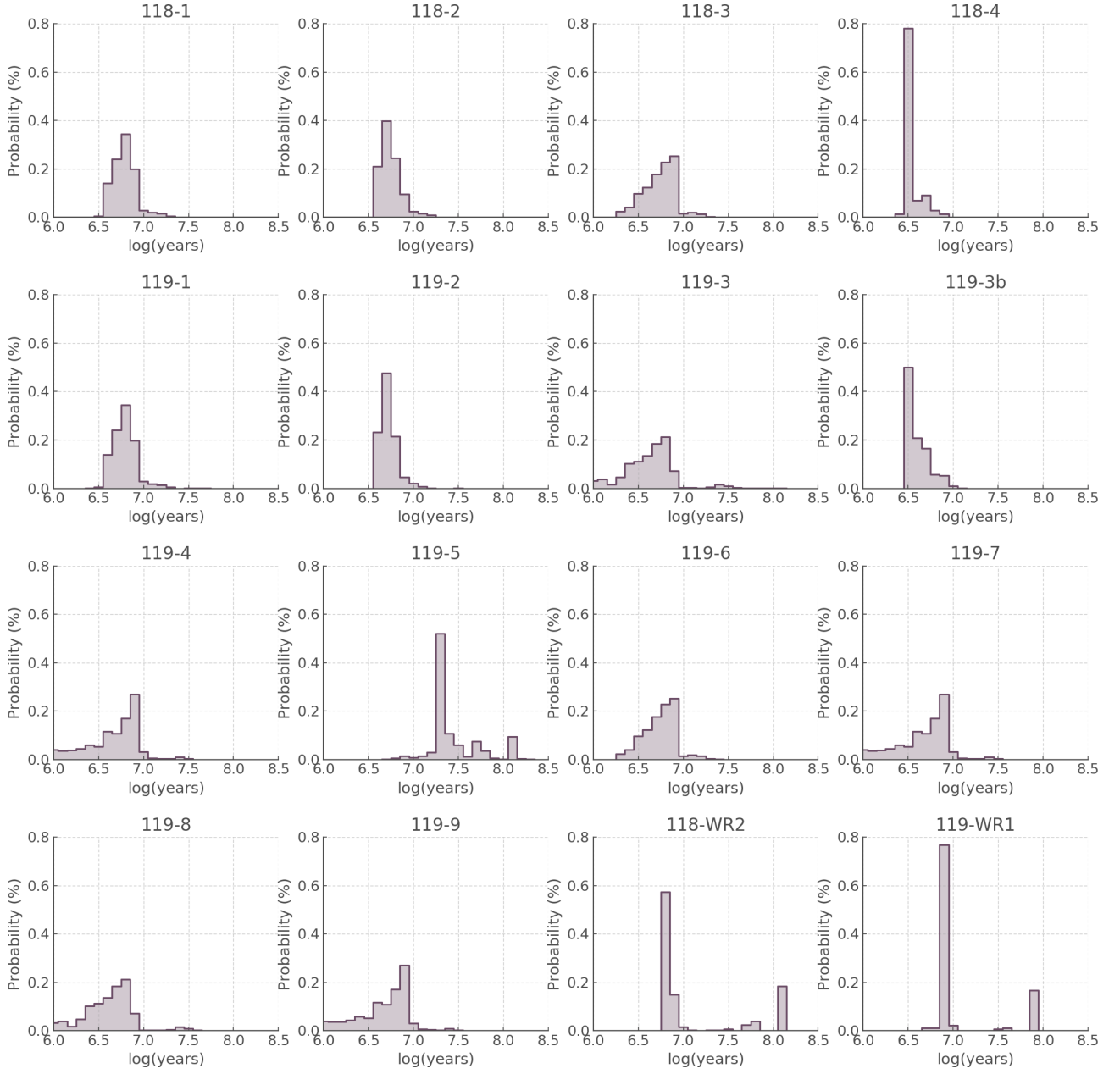


**Figure A2.** Same as Figure A1 for a metallicity  $Z = 0.08$ .



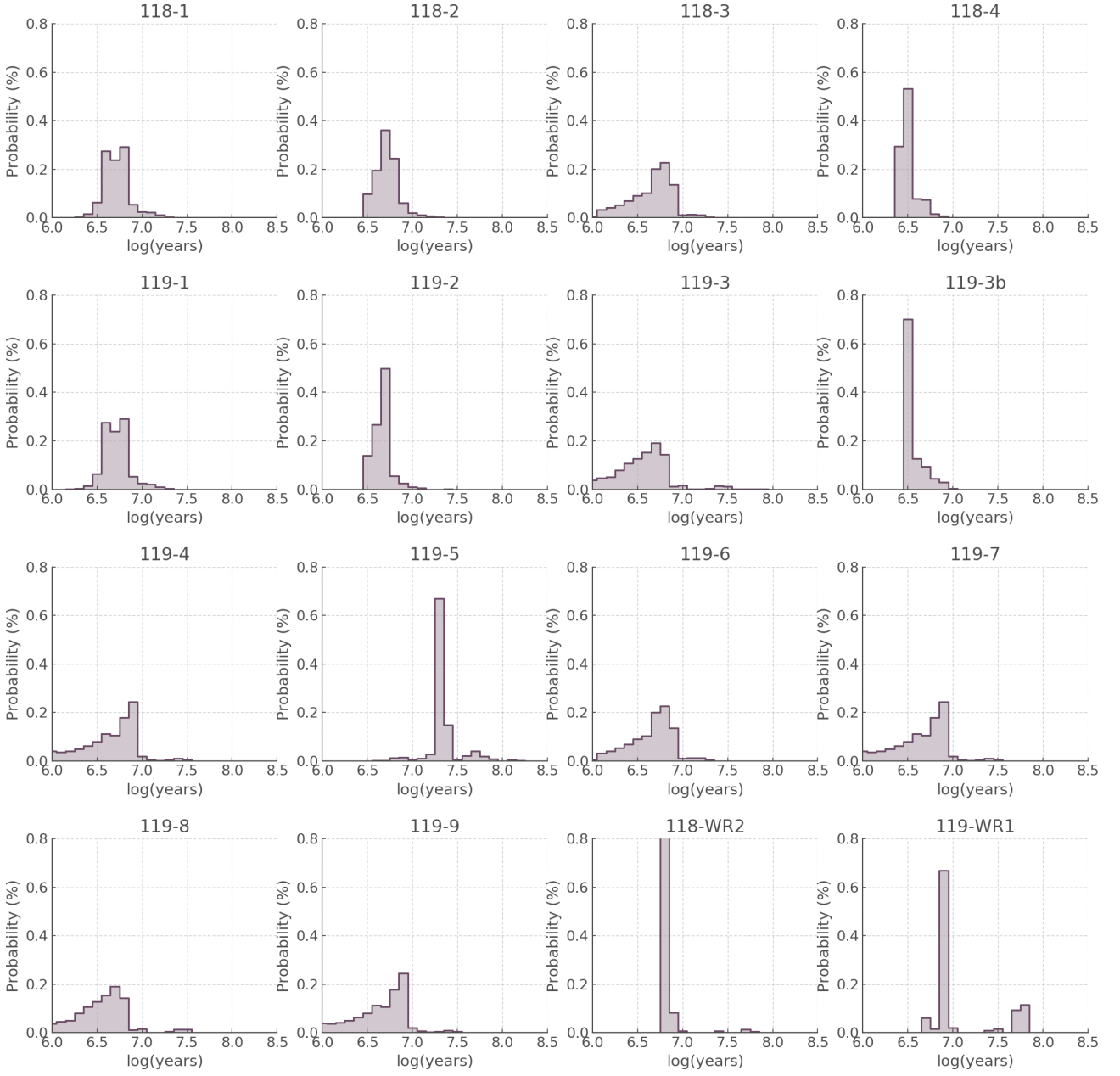


**Figure A3.** Same as Figure A1 for a metallicity  $Z = 0.10$  or half solar.